Correlation of Maximum Temperature Increase and Peak SAR in the Human Head Due to Handset Antennas

Akimasa Hirata, *Member, IEEE,* and Toshiyuki Shiozawa, *Fellow, IEEE*

***Abstract*—This paper attempts to correlate the maximum temperature increase in the head and brain with the peak specific absorption rate (SAR) value due to handset antennas. The rationale for this study is that physiological effects and damage to humans through electromagnetic-wave exposure are induced by temperature increases, while the safety standards are regulated in terms of the local peak SAR. For investigating these correlations thoroughly, the total of 660 situations is considered. The numerical results are analyzed on the basis of statistics. We find that the maximum temperature increases in the head and brain can be estimated in terms of peak SARs averaged over 1 and 10 g of tissue in these regions. These correlations are less affected by the positions, polarizations, and frequencies of a dipole antenna. Also, they are reasonably valid for different antennas and head models. Further, we discuss possible maximum temperature increases in the head and brain for the SAR values prescribed in the safety standards. They are found to be 0.31 °C and 0.13 °C for the Federal Communications Commission Standard (1.6 W/kg for 1 g of tissue), while 0.60 °C and 0.25 °C for the International Commission on Non-Ionizing Radiation Protection Standard (2.0 W/kg for 10 g of tissue).**

***Index Terms*—Dosimetry, finite-difference time-domain (FDTD) method, specific absorption rate (SAR), temperature increase.**

I. Introduction

In RECENT years, there has been an increasing public concern about the health implications of electromagnetic (EM) wave exposure with the use of mobile telephones [1]. Therefore, various organizations throughout the world have established safety guidelines for EM wave absorption [2]–[4]. For RF near-field exposure, these standards are based on the spatial peak specific absorption rate (SAR) for any 1 or 10 g of body tissue. However, physiological effects and damage to humans by EM-wave exposures are induced by temperature increases. A temperature increase of 4.5 °C in the brain has been noted to be an allowable limit, which does not lead to any physiological damage (for exposures of more than 30 min) [5]. Additionally, the threshold temperature of the pricking pain in skin is 45 °C, corresponding to the temperature increase of 10 °C–15 °C [6], [7]. Therefore, the temperature increase in the anatomically based human-head model for exposure to EM waves from handset antennas has been calculated in several papers [8]–[15]. According to these papers, the temperature increase distribution in the human head is largely affected by the SAR distribution, and the former is not linearly proportional to the latter. This is attributed to heat diffusion. The nonlinear relation between the SAR and temperature increase distributions has made many authors further investigate the temperature increase in the head due to handset antennas. In these papers, however, sufficient attention has not been paid to the correlation between peak SARs (averaged over 1 or 10 g of tissue) and maximum temperature increases in the head and brain. One of the main reasons for this is that only a limited number of situations were considered because of the large computational cost. This being the case, we have presented a hypothesis [16] that maximum temperature increases in the head and brain are reasonably proportional to peak SARs in these regions. This hypothesis is roughly formulated on the basis of the results of only ten situations, which correspond to five frequencies, together with two polarizations.

In this paper, we thoroughly discuss the correlation between peak SARs and maximum temperature increases in the head and brain, and clarify the validity of our hypothesis. In our investigation, the total of 660 cases is considered, and sets of peak SARs and maximum temperature increases are processed on the basis of statistics. It should be noted that, in this paper, the intrinsic temperature increase in the head due to EM-wave exposure is discussed. In other words, no attention is paid to the temperature increase due to a handset itself, which is warmed by internal electronic circuits, unlike the previous work [15].

The calculation procedure for the SAR and temperature increase in the head is the same as [8]–[13], [15] in that: 1) the SAR in the head is calculated by using the FDTD method and 2) the temperature increase in the head is calculated with the use of FD method by substituting the SAR obtained in 1) into the bioheat equation [17].

II. Model and Method for the Analysis

A. Human-Head Model

The human-head model used in this paper is almost the same as that developed in [18], except for some minor modifications. It consists of $96 \times 110 \times 125$ cubic cells, whose side cell length is 2.0 mm. This model is comprised of 18 tissues, i.e., bone (skull), cartilage, cornea, sclera, lens, aqueous humor, vitreous humor, muscle, skin, fat, white matter, grey matter, cerebellum, dura, nerve, tongue, cerebrospinal fluid (CSF), and blood. At the frequency of 2.45 GHz, each cell in this model is subdivided into eight cubic cells comprised of the same tissue with a side length

Manuscript received October 30, 2002; revised March 5, 2003. This work was supported in part by the Telecommunications Advancement Foundation.

The authors are with the Department of Communication Engineering, Osaka University, Osaka 565-0871, Japan (e-mail: hirata@comm.eng.osaka-u.ac.jp).

Digital Object Identifier 10.1109/TMTT.2003.814314

of 1.0 mm in order to suppress numerical dispersion error below 1%: the cell side length should be smaller than $\lambda_{\min}/10$, where $\lambda_{\min}$ is the shortest wavelength in the system [19]. In addition to our model, the model constructed by Brooks Air Force Base[1] is also used to discuss some uncertainties due to different models.

B. Finite-Difference Time-Domain (FDTD) Method

The FDTD method [19] is used for investigating the interaction between the human-head model and handset antennas. In order to incorporate the inhomogeneous head model into the FDTD scheme, the dielectric properties of the tissues are required. They are determined with the aid of the 4–Cole–Cole extrapolation [20]. For geometries in which wave–object interaction has to be considered in the open region, the computational space has to be truncated by absorbing boundaries ([19, Ch. 7]). In this paper, an eight-layer Berenger's perfectly matched layer (PML) [21] with a parabolic profile is adopted as the absorbing boundary.

C. SAR Calculation

For harmonically varying EM fields, the SAR is defined as

$$\mathrm{SAR} = \frac{\sigma}{2\rho}|\hat{E}|^2 = \frac{\sigma}{2\rho}\left(|\hat{E}_x|^2 + |\hat{E}_y|^2 + |\hat{E}_z|^2\right) \quad (1)$$

where $\hat{E}_x$, $\hat{E}_y$, and $\hat{E}_z$ are the peak values of electric-field components, σ and ρ denoting the conductivity and mass density of the tissue. The 12-component approach is used for obtaining SARs [22] in each cell. For the shape of the averaging volume, we choose a cube. Note that 10% air inclusion is allowed for calculating the peak SARs averaged over 1 and 10 g of tissues in the head. Similarly, other tissues are included by less than 10% for the calculation of peak SARs for the brain tissue. Here, we define the brain as composed of white matter, gray matter, cerebellum, dura, and CSF

D. Temperature Increase Calculation

Only the outline of the algorithm for calculating the temperature increase is described since our procedures are the same as those in [8]–[13] and [23]. For calculating the temperature increase in the human head, the bioheat equation [17], which takes into account the heat exchange mechanisms such as heat conduction, blood flow, and EM heating, is used. The bioheat equation is represented as

$$C\rho\frac{dT}{dt} = K\nabla^2 T + \rho(\mathrm{SAR}) - BT \quad (2)$$

where T is the temperature increase of the tissue, K is the thermal conductivity of the tissue, C is the heat capacity of the tissue, and B is the term associated with blood flow. In addition, the boundary condition for (2) is given by

$$H \cdot (T_s - T_c) = -K\frac{\partial T}{\partial n} \quad (3)$$

where H, T_s, and T_e denote, respectively, the convection coefficient, surface temperature, and temperature of the air. The finite-difference expressions for (2) and (3) are given in [9], [13], and [23].

[1][Online]. Available: http://www.brooks.af.mil/AFRL/HED/hedr/hedr.html

TABLE I
THERMAL PROPERTIES OF TISSUES IN THE HUMAN HEAD

Tissues	C_t [J/kg· °C]	K [W/m· °C]	B [W/m^3·°C]
Skin	3500	0.42	9100
Muscle	3600	0.50	2700
Bone	1300	0.40	1000
Blood	3900	0.49	0
Fat	2500	0.25	520
Grey Matter	3700	0.57	35000
White Matter	3600	0.50	35000
Cerebellum	4200	0.58	35000
Humor	4000	0.60	0
Lens	3000	0.40	0
Sclera/Cornea	4200	0.58	0
C.S.F.	4000	0.60	0
Tongue	3300	0.42	13000
Brain Dura	3600	0.50	2700

At the initial state, the steady-state temperature distribution in the head is given. This distribution is obtained from the steady-state bioheat equation

$$K\nabla^2 T - BT = 0 \quad (4)$$

subject to boundary conditions (3) with the assumption that the body core temperature is 37.0 °C. We then follow the temperature increase by solving (2) until we reach a steady state (for approximately 30 min [13]).

The thermal parameters of tissues are listed in Table I [5], [24]–[29]. In this table, most of the material constants are borrowed from [13, Table II] for comparison with the results in that paper. It should be noticed that the results based on animal experiments are used for most of the thermal parameters because we have no reliable actual data available for the parameters required in the human-head model. The uncertainties in the maximum temperature increases caused by those in thermal parameters can be found in [16].

III. CORRELATION BETWEEN AVERAGE SARS AND TEMPERATURE INCREASES

A. Hypothesis and Evaluation Scheme

Wang *et al.* showed numerically that the temperature increase in the human head due to a monopole antenna is almost linearly proportional to the output power [12]. Let us consider the physical meaning of this relation in short. At *the thermal steady state*, (2) is reduced to the following:

$$K\nabla^2 T + \rho(\mathrm{SAR}) - BT = 0. \quad (5)$$

This is a linear equation in terms of T and, thus, the steady-state temperature increase in the head is proportional to the SAR (or the output power of the handset antenna). Note that *transient* distribution of the temperature increase is not proportional to the output power. When the maximum temperature increase is considered at the thermal steady state, it could be appropriate to

express the maximum temperature increase in the head or brain approximately as the following equation:

$$\hat{T} = a \cdot \mathrm{SAR}_{\mathrm{ave}} \tag{6}$$

where $\mathrm{SAR}_{\mathrm{ave}}$, $\hat{T}$, and a denote, respectively, the peak SAR averaged over 1 or 10 g of tissue in the head or brain, the maximum temperature increase estimated by the regression line, and the slope of the regression line with the unit of °C · Kg/W, which are determined by using the method of least squares [30]. Note that the intercept of the regression line is set to zero since no temperature increase in the head is induced without EM power absorption. It is this relation that we presented in [16] as the hypothesis. It should be noted that we have confirmed the linear temperature increase in the head and brain with the increase of the output power of the antenna in the frequency range between 900 MHz–2.5 GHz [16]. In additiona, the maximum temperature increase in the head is so defined as to exclude the auricles. This is because the peak SAR averaged over 1 or 10 g of tissue does not appear in the auricle due to its complex shape. Consequently, it is difficult to correlate the maximum temperature increase appearing in auricle and the peak 1- or 10-g SAR in the head [16].

For evaluating the effectiveness of the estimation scheme for the maximum temperature increase, the coefficient of determination r^2 is introduced as

$$r^2 = \frac{\sum_i \left(\hat{T}_i - \bar{T}\right)^2}{\sum_i \left(T_i - \bar{T}\right)^2} = 1 - \frac{\sum_i \left(T_i - \hat{T}_i\right)^2}{\sum_i \left(T_i - \bar{T}\right)^2} \tag{7}$$

where T_i is the maximum temperature increase for the ith case, and $\bar{T}$ is the mean value of T_i. Note that the value of coefficient of determination increases with the increase of the number of samples n. Thus, the coefficient should be adjusted in accordance with the degrees of freedom. The adjusted coefficient is defined as

$$\bar{r}^2 = 1 - \frac{n-1}{n-2}\left(1 - r^2\right). \tag{8}$$

It should be noted that $\bar{r}^2$ can be considered a measure of how well the regression line agrees with the observed values [30], [31]. Namely, the less the observed values depart from the fitted line, the smaller the second term in (8) is and the closer to unity $\bar{r}^2$ is. When the value of $\bar{r}^2$ becomes negative, the value of $\bar{r}^2$ is set to 0. This corresponds to the case that no clear correlation is observed between the maximum temperature increase and the peak SAR.

B. Effectiveness of the Estimation Scheme

The effectiveness of the correlation scheme between the maximum temperature increase and peak SAR values are discussed for a dipole antenna. The following total of 360 situations is considered:

- head models with pressed or unpressed ear;
- five frequencies: 900 MHz and 1.5, 1.9, 2.1, and 2.45 GHz;
- two polarizations: the horizontal polarization (HP) and vertical polarization (VP);
- 18 feeding points (see Fig. 1).

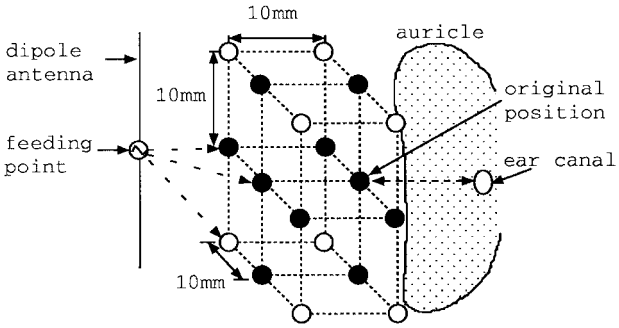

Fig. 1. Positions for the feeding points of the dipole antenna relative to the auricle; both points ∘ and points • denote 18 feeding positions, and points • denote ten positions. The distance between the original feeding point and ear canal is 26 mm.

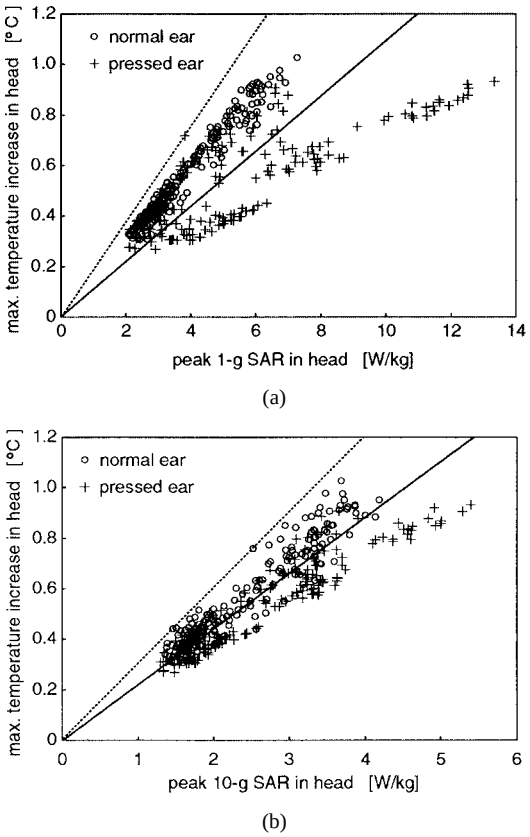

Fig. 2. Maximum temperature increase in the head versus SAR averaged over: (a) 1- and (b) 10-g tissues in the head. The regression line and the line indicating the maximum slope are demonstrated by solid and dotted lines.

The thickness of unpressed and pressed ears is 18 and 6 mm, respectively. The diameter of the dipole antenna is fixed to 1.0 mm, but the length takes several values: 160, 92, 72, 64, and 54 mm for 900 MHz and 1.5, 1.9, 2.15, and 2.45 GHz, respectively.

Fig. 2(a) and (b) illustrates the relation between the peak 1- or 10-g SAR in the head and the maximum temperature increase in the head. In this figure, the regression line and the line indicating the maximum slope are demonstrated by solid and dotted lines. As seen from the figure, the maximum temperature increase in the head is reasonably proportional to the peak SAR averaged over 10 g of tissue. In particular, it is not found to be dependent on the frequency (see also Table II). On the other hand, the peak

TABLE II
ESTIMATED SLOPE (°C · Kg/W) AND THE ADJUSTED COEFFICIENT OF DETERMINATION FOR THE MAXIMUM TEMPERATURE INCREASE IN THE HUMAN HEAD VERSUS THE PEAK SARS IN THE HEAD

	1g SAR [W/kg]		10g SAR [W/kg]	
	a	$\bar{r}^2$	a	$\bar{r}^2$
Pressed	0.091	0.250	0.197	0.867
Normal	0.147	0.962	0.237	0.906
All	0.109	0.132	0.215	0.804

1-g SAR in the head cannot be reasonably correlated with the maximum temperature increase in the head. As is evident from Fig. 2(a), this is due to the effect of ear shape, i.e., the plots for the head with the normal ear are well on its own regression line, while those for the pressed ear are dispersed (see Table II). This is mainly caused by the relative position of peak SARs and maximum temperature increase: for the model with the pressed ear, the position of maximum temperature increase is close to that of the peak 10-g SAR, while it is not always the case for the peak 1-g SAR. For the model with the normal ear, the positions of peak SARs and maximum temperature increase almost coincide for most samples. It is worth noting that our results present the following features clarified in the previous papers: 1) the peak 1- and 10-g SARs appear near auricle for the model with the *lossy* ear [32] and 2) the positions of peak 1- and 10-g SARs do not always appear in close proximity to one another [33]. The point to be stressed is that the regression line for the peak 10-g SAR in the head could be effective since the averaging scheme, SAR distribution, curvature of the actual head models, and so on affect the peak SAR by as much as 20%–30% [22], [34], [35].

Fig. 3 shows the maximum temperature increases in the brain versus the peak SARs averaged over 1 and 10 g of tissues in the head. As seen from this figure, the plots are dispersed, and little correlation can be observed. It is expected from the discussion above and in [16] that an accurate correlation cannot be obtained in cases where the position of the maximum temperature increase is not involved in the averaging volumes of peak SARs for the majority of samples. It should be noted that the maximum temperature increase in the brain appears around the boundary between the skull and brain, as can be seen in [9], [13], and [16].

It is interesting to illustrate the maximum temperature increase in the brain versus the peak 1- and 10-g SARs in the brain (Fig. 4). From this figure, the maximum temperature increase in the brain is extrapolated by using either one of the peak 1- or 10-g SARs in the brain. For evaluating the effectiveness of the estimation scheme for the maximum temperature increase in terms of peak SAR quantitatively, the slope a in (6) and the adjusted coefficient of determination are listed in Table III, together with the case where the average SARs in the head are used. From this table, we find that the SAR averaged over 1 g of brain tissue enables us to estimate the maximum temperature increase with better accuracy than the peak 10-g SAR of the brain. This is because the heat evolved in the brain is much diffused due to the large blood flow, as compared with the other tissues. Thus, the temperature increase distribu-

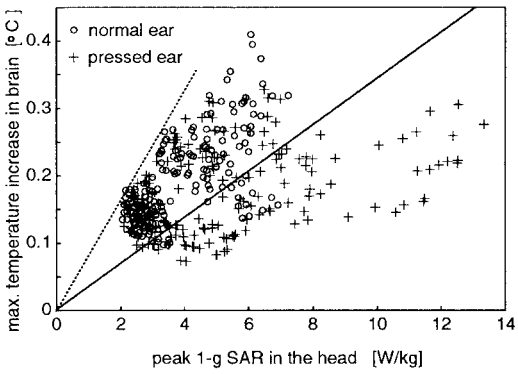

(a)

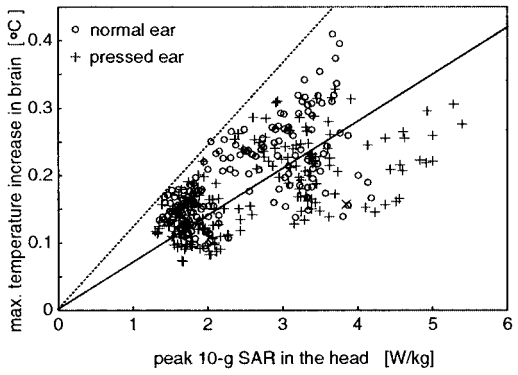

(b)

Fig. 3. Maximum temperature increase in the brain versus SAR averaged over: (a) 1- and (b) 10-g tissue in the head. The regression line and the line indicating the maximum slope are demonstrated by solid and dotted lines.

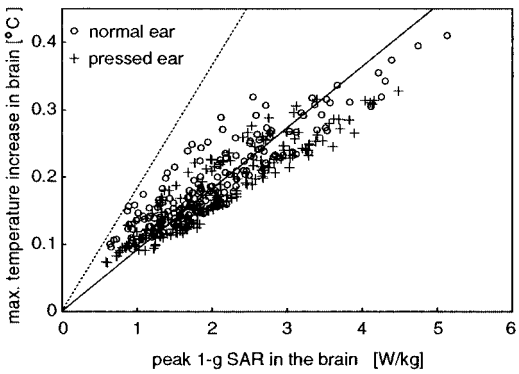

(a)

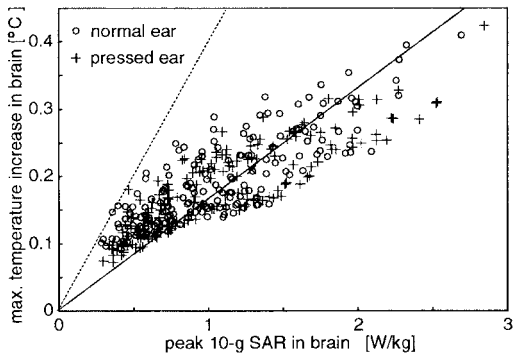

(b)

Fig. 4. Maximum temperature increase in the brain versus SAR averaged over: (a) 1- and (b) 10-g tissue in the brain. The regression line and the line indicating the maximum slope are demonstrated by solid and dotted lines.

TABLE III
ESTIMATED SLOPE (°C · Kg/W) AND THE ADJUSTED COEFFICIENT OF DETERMINATION FOR: (a) THE MAXIMUM TEMPERATURE INCREASE IN THE BRAIN VERSUS PEAK SAR IN THE HEAD AND (b) THE MAXIMUM TEMPERATURE INCREASE IN THE BRAIN VERSUS PEAK SAR IN THE BRAIN

	1g SAR [W/kg]		10g SAR [W/kg]	
	a	$\bar{r}^2$	a	$\bar{r}^2$
Pressed	0.028	0	0.064	0.280
Normal	0.048	0.341	0.078	0.387
All	0.035	0	0.070	0.260

(a)

	1g SAR [W/kg]		10g SAR [W/kg]	
	a	$\bar{r}^2$	a	$\bar{r}^2$
Pressed	0.084	0.778	0.156	0.493
Normal	0.091	0.729	0.169	0.470
All	0.088	0.738	0.163	0.474

(b)

tion in the brain is largely affected not only by the SAR in the averaging volume, but also by the SAR distribution and blood flow in the surrounding region. Consequently, the uncertainty in the estimation is increased by the blood flow when treating a larger volume in the brain. It should be noted that the positions of maximum temperature increase and peak SARs in the brain coincide reasonably for the majority of samples. They appear at the outer boundary of the brain. If we choose a cube for the SAR averaging, the position of maximum temperature increase appears on the side close to the antenna.

C. Effect of Different Antennas on the Slope a

In order to clarify the effect of different antennas on the slope a in (6), our head model with the pressed ear is used. Since it has been shown that maximum temperature increases in the head and brain were well estimated by using the peak 10- and 1-g SARs in the corresponding regions, attention is paid only to these correlations. The following total of 300 situations are considered:

- three antennas: an isolated dipole antenna (see Fig. 1), monopole, and helical antennas on a metallic box (see Fig. 5);
- two polarizations: the HP and VP;
- five frequencies: 900 MHz and 1.5, 1.9, 2.1, and 2.45 GHz;
- ten feeding points (see Fig. 5).

For all the above cases, the dimension of the metallic box is 20 mm × 40 mm × 104 mm. It should be noted that the metallic box is coated with a dielectric (relative permittivity $= 1.6$) with the thickness of 2.0 mm. This box touches the edge of the auricle when considering the original position (see Fig. 1) as a feeding point. The diameter of the monopole is fixed to 1.0 mm, but the length d takes values of 80, 46, 36, 32, and 27 mm for 900 MHz and 1.5, 1.9, 2.15, and 2.45 GHz, respectively. For the helical antenna, the diameter and pitch of the helix are fixed to 4.0 and 2.0 mm, and its length is 28, 18, 14, 12, and 10 mm for 900 MHz and 1.5, 1.9, 2.15, and 2.45 GHz.

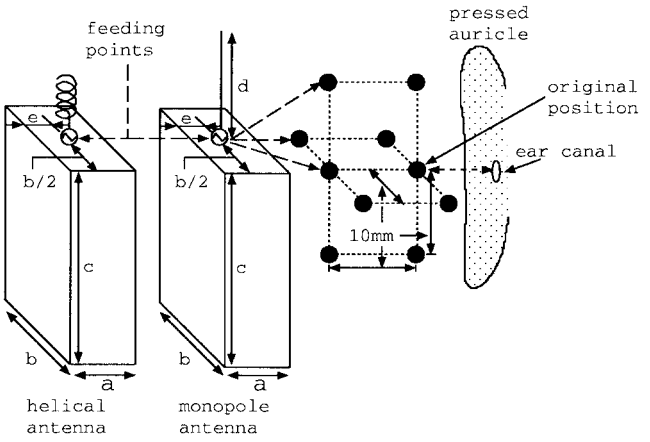

Fig. 5. Positions for the feeding point of the monopole and helical antennas on the metallic box relative to the pressed ear: $a = 20$ mm, $b = 40$ mm, $c = 104$ mm, and $e = 2.0$ mm. The distance between the original position and ear canal is 26 mm.

TABLE IV
EFFECT OF DIFFERENT ANTENNAS ON THE ESTIMATION PARAMETERS

	head (10g SAR)		brain (1g SAR)	
	a	$\bar{r}^2$	a	$\bar{r}^2$
Dipole	0.196	0.890	0.083	0.798
Monopole	0.192	0.962	0.092	0.785
Helical	0.187	0.975	0.102	0.905
All	0.193	0.923	0.088	0.780

Table IV shows the slope a and the adjusted coefficient of determination for each antenna. As is evident from this table, the effect of different antennas on the estimation parameters for the head is small. On the other hand, the slope of the estimation for the brain is affected by the antenna shape, but it is at most 20%. It should be noted that the adjusted coefficient of determination $\bar{r}^2$ for the brain obtained for the helical antenna is closer to unity than for the others. The main reason for this is that the SAR distribution is concentrated around a particular region near the antenna feeding point, which is caused by the shape of the antenna [36]. As a result, the SAR distribution decreases rapidly as going away from the position where the peak SAR appears. Namely, the heat evolved in the volume of the peak 1-g SAR in the brain becomes much larger than that evolved in the surrounding region. Thus, the maximum temperature increase for the helical antenna is less affected by blood flow than for the other antennas, as can be expected from (5). It is noteworthy that the positions of peak SARs and the maximum temperature increase in the head appear near the auricle for the monopole and helical antennas, as well as for the dipole antenna.

D. Effect of Different Head Models on the Slope a

In order to discuss some uncertainty in the slope a due to the difference in head models, the models constructed by our group and the Brooks AFB are considered. The following total of 200 situations is considered for the dipole antenna:

- two head models (by Osaka University, Osaka, Japan, and Brooks Air Force Base, Brooks AFB, TX);

TABLE V
EFFECT OF DIFFERENT HEAD MODELS ON ESTIMATION PARAMETERS

	head(10g SAR)		brain (1g SAR)	
	a	$\bar{r}^2$	a	$\bar{r}^2$
Our model	0.198	0.847	0.084	0.778
Brooks model	0.185	0.542	0.207	0.689
Results in [13]	0.197	0.697	0.116	0.736

- five frequencies: 900 MHz and 1.5, 1.9, 2.1, and 2.45 GHz;
- two polarizations: the HP and VP;
- ten feeding points.

Table V shows the slope a and the adjusted coefficient of determination for each model. In addition, the results in [13] are also shown for comparison, although only ten samples are listed in the reference.[2] From this table, it is found that the maximum temperature increases in the head and brain can be reasonably estimated in terms of peak SAR even for the Brooks model. Furthermore, the slope for the peak 10-g SAR versus the maximum temperature increase in the head is almost the same for all models. On the other hand, the slope for the brain is largely dependent on models. We observe that the main reason for this is the difference in the structure of the head models around the ear. It is worth noting that the results in [37] for the temperature increase in the brain reasonably agree with our results (within 10%–20% for four samples).

E. Maximum Temperature Increase for the SAR Prescribed in Safety Standards

This section discusses maximum temperature increases in the head and brain for the SAR limits prescribed in the safety standards. The upper limit for near-field exposures in public environments is 1.6 W/kg for any tissue averaged over 1 g in the Federal Communications Commission (FCC) Standard [2], while it is 2.0 W/kg for 10 g of tissue in the International Commission on Non-Ionizing Radiation Protection (ICNIRP) Standard [4]. Table VI shows maximum values of possible temperature increases in the head and brain for the SAR value prescribed in the standards, together with those in the previous papers. Note that maximum values of possible temperature increases are defined on the basis of the maximum slopes in Figs. 2 and 3. Namely, they are defined as the product of the SAR limit in the standards and the maximum slope. It is noteworthy that this slope is little affected by the kind of antennas, although they are not shown to avoid similar repetition. As seen from this table, the maximum values of possible temperature increase in the head and brain are 0.31 °C and 0.13 °C for the FCC Standard, while 0.60 °C and 0.25 °C for the ICNIRP Standard. From the viewpoint of maximum temperature increase, the ICNIRP Standard is less stringent than the FCC Standard by a factor of two. This agrees well for our results using the Brooks model. On the other hand, a somewhat large temperature increase is observed in the maximum temperature increase in the head as shown in Table VI(e). This might be because we define the maximum temperature increase in the head excluding the auricle, while the other authors have possibly defined it including the auricle (although no clear description was given).

[2]At least 50 samples are required for proper statistical approach.

TABLE VI
POSSIBLE MAXIMUM TEMPERATURE INCREASES (°C) DUE TO THE DIPOLE ANTENNA: OUR RESULTS WITH THE USE OF: (a) OUR MODEL AND (b) THE BROOKS MODEL, AND THE RESULTS (c) IN [8], (d) IN [13], AND (e) IN [14]

		head	brain
(a)	FCC	0.31	0.13
	ICNIRP	0.60	0.25
(b)	FCC	0.28	0.08
	ICNIRP	0.64	0.20
(c)	FCC	0.25	0.17
	ICNIRP	0.42	0.26
(d)	FCC	0.23	0.14
	ICNIRP	0.53	0.24
(e)	FCC	0.30	0.13
	ICNIRP	0.92	0.33

IV. SUMMARY

In this paper, we have attempted to correlate the maximum temperature increase in the head and brain with the peak SAR averaged over 1 and 10 g of tissues due to handset antennas. The rationale for this study was that physiological effects and damage to humans due to EM wave exposure are induced through temperature increases, although the safety standards are regulated in terms of the peak SARs. For investigating these correlations thoroughly, we considered the total of 660 different situations. The numerical results for these cases were analyzed on the basis of statistics. For the result of our investigations, we have found that maximum temperature increases in the head and brain can be estimated in terms of peak SARs averaged over 10 g of tissue and 1 g of tissue in these regions. These correlations were less affected by the positions, polarizations, and frequencies of the dipole antenna. Also, they were found to be valid for different antennas. Furthermore, the slopes to correlate the maximum temperature increase in the head and the peak 10-g SAR in the head were almost identical for different head models (within 10%). On the other hand, the slopes correlating the maximum temperature increase in the brain and the peak 1-g SAR in the brain were largely affected by the head models (up to 100%), although the linear correlation is valid for all head models.

From the results for the dipole antenna (360 situations), we discussed maximum values of possible temperature increases in the head and brain for the SAR values prescribed in the safety standards. They are 0.31 °C and 0.13 °C for the FCC Standard (1.6 W/kg for 1 g of tissue), while they are 0.60 °C and 0.25 °C for the ICNIRP Standard (2.0 W/kg for 10 g of tissue). These results are comparable with those in previous papers. It is worth noting that these temperature increases are well within normal biological variations of temperature in humans [38].

ACKNOWLEDGMENT

The authors would like to thank M. Morita, Osaka University, Osaka, Japan, for his assistance in this study and Prof. O. Fujiwara, Nagoya Institute of Technology, Nagoya, Japan, for his valuable comments on this study. The authors would also like to thank Dr. S. Watanabe and S. Mochizuki, both of the Communication Research Laboratory, Tokyo, Japan, for giving their notes on the effect of auricle on SAR, and the anonymous reviewers for their kind suggestions.

REFERENCES

[1] M. Burkhardt and N. Kuster, "Review of exposure assessment for handheld mobile communications devices and antenna studies for optimized performance," in *Review of Radio Science 1996–1999*, W. R. Stone, Ed. Oxford, U.K.: Oxford Univ. Press, 1999, ch. 34.

[2] "Evaluating compliance with FCC guidelines for human exposure to radio frequency electromagnetic fields," FCC, Washington, DC, Tech. Rep. OET Bulletin 65, 1997.

[3] "Radio-radiation protection guidelines for human exposure to electromagnetic fields," Telecommun. Technol. Council Ministry Posts Telecommun., Tokyo, Japan, Deliberation Rep. 89, 1997.

[4] International Commission on Non-Ionizing Radiation Protection (ICNIRP), "Guidelines for limiting exposure to time-varying electric, magnetic and electromagnetic fields (up to 300 GHz)," *Health Phys.*, vol. 74, pp. 494–522, 1998.

[5] A. C. Guyton and J. E. Hall, *Textbook of Medical Physiology*. Philadelphia, PA: Saunders, 1996.

[6] J. D. Hardy, H. G. Wolff, and H. Goodell, *Pain Sensations and Reactions*. Baltimore, MD: Williams & Wilkins, 1952, ch. IV and X.

[7] J. D. Hardy, "The nature of pain," *J. Chronic Dis.*, vol. 4, no. 22, 1956.

[8] G. M. J. Van Leeuwen, J. J. W. Lagendijk, B. J. A. M. Van Leersum, A. P. M. Zwamborn, S. N. Hornsleth, and A. N. T. Kotte, "Calculation of change in brain temperatures due to exposure to a mobile phone," *Phys. Med. Biol.*, vol. 44, pp. 2367–2379, 1999.

[9] J. Wang and O. Fujiwara, "FDTD computation of temperature rise in the human head for portable telephones," *IEEE Trans. Microwave Theory Tech.*, vol. 47, pp. 1528–1534, Aug. 1999.

[10] A. Hirata, T. Katayama, and T. Shiozawa, "Thermal effects in the human head for exposure to EM waves emitted from terminals for mobile satellite services," in *Proc. 10th IEEE Int. Personal Indoor and Mobile Radio Communications Symp.*, Osaka, Japan, Sept. 1999, Paper G-5-4.

[11] M. Morita, A. Hirata, and T. Shiozawa, "Temperature rises in the human head exposed to EM waves emitted from a dipole antenna at various microwave frequencies," in *Proc. Optical Fiber Science and Electromagnetic Theory*, Osaka, Japan, Dec. 2000, pp. 283–286.

[12] J. Wang, T. Joukou, and O. Fujiwara, "Dependence of antenna output power of temperature rise in human head for portable telephones," in *Proc. Asia–Pacific Microwave Conf.*, vol. 2, Nov. 1999, pp. 481–484.

[13] P. Bernardi, M. Cavagnaro, S. Pisa, and E. Piuzzi, "Specific absorption rate and temperature increases in the head of a cellular-phone user," *IEEE Trans. Microwave Theory Tech.*, vol. 48, pp. 1118–1126, July 2000.

[14] P. Wainwright, "Thermal effects of radiation from cellular telephones," *Phys. Med. Biol.*, vol. 45, pp. 2363–2372, 2000.

[15] O. P. Gandhi, Q.-X. Li, and G. Kang, "Temperature rise for the human head for cellular telephones and for peak SARs prescribed in safety guidelines," *IEEE Trans. Microwave Theory Tech.*, vol. 49, pp. 1607–1613, Sept. 2001.

[16] A. Hirata, M. Morita, and T. Shiozawa, "Temperature increase in the human head due to a dipole antenna at microwave frequencies," *IEEE Trans. Electromagn. Compat.*, vol. 45, pp. 109–117, Feb. 2003.

[17] H. H. Pennes, "Analysis of tissue and arterial blood temperature in resting forearm," *J. Appl. Phys.*, vol. 1, pp. 93–122, 1948.

[18] A. Hirata, S. Matsuyama, and T. Shiozawa, "Temperature rises in the human eye exposed to EM waves in the frequency range 0.6–6 GHz," *IEEE Trans. Electromagn. Compat.*, vol. 42, pp. 386–393, Nov. 2000.

[19] A. Taflove and S. Hagness, *Computational Electrodynamics: The Finite-Difference Time-Domain Method*, 2nd ed. Norwood, MA: Artech House, 1995.

[20] "Final technical report occupational and environmental health directorate," RFR Div., Brooks Air Force Base, Brooks AFB, TX, AL/OE-TR-1996-0037, 1996.

[21] J. P. Berenger, "A perfectly matched layer for the absorption of electromagnetic wave," *J. Comput. Phys.*, vol. 114, pp. 185–200, 1994.

[22] K. Caputa, M. Okoniewski, and M. Stuchly, "An algorithm for computation of the power deposition in human tissue," *IEEE Antennas Propagat. Mag.*, vol. 41, pp. 102–107, June 1999.

[23] A. Taflove and M. E. Brodwin, "Computation of the electromagnetic fields and induced temperatures within a model of the microwave-irradiated human eye," *IEEE Trans. Microwave Theory Tech.*, vol. MTT-23, pp. 888–896, Nov. 1975.

[24] F. A. Duck, *Physical Properties of Tissue*. New York: Academic, 1990.

[25] J. J. Lagendijk, "A mathematical model to calculate temperature distributions in human and rabbit eyes during hyperthermic treatment," *Phys. Med. Biol.*, vol. 27, no. 11, pp. 1301–1311, 1982.

[26] J. A. Scott, "A finite element model of heat transport in the human eye," *Phys. Med. Biol.*, vol. 33, no. 2, pp. 227–241, 1988.

[27] L. R. Williams and R. W. Leggett, "Reference values for resting blood flow to organs of man," *Clinical Phys. Physiol. Meas.*, vol. 10, no. 3, pp. 187–217, 1989.

[28] R. G. Gordon, R. B. Roemer, and S. M. Horvath, "A mathematical model of the human temperature regulatory system—Transient cold exposure response," *IEEE Trans. Biomed. Eng.*, vol. BME-23, pp. 434–444, 1976.

[29] R. J. Dickinson, "An ultrasound system for local hypothermia using scanned focused transducers," *IEEE Trans. Biomed. Eng.*, vol. BME-31, pp. 120–125, 1984.

[30] L. Sachs, *Applied Statistics: A Handbook of Techniques*, 2nd ed. New York: Springer Verlag, 1982.

[31] L. L. Lapin, *Statistics: Meaning & Method*. New York: Harcourt Brace Jovanovich, 1975.

[32] S. Watanabe, H. Wakayanagi, T. Hamada, M. Taki, Y. Yamanaka, and H. Shirai, "The peak SAR in a human head that has an earlobe exposed to microwave from a cellular telephone," in *Proc. XXVI General Assembly of URSI*, Toronto, ON, Canada, Aug. 1999, p. 847.

[33] M. Burkhart and N. Kuster, "Appropriate modeling of the ear for compliance testing of handheld MTE with SAR safety limits at 900/1800 MHz," *IEEE Trans. Microwave Theory Tech.*, vol. 48, pp. 1927–1934, Nov. 2000.

[34] N. Stevens and L. Martens, "Comparison of averaging procedures for SAR distributions at 900 and 1800 MHz," *IEEE Trans. Microwave Theory Tech.*, vol. 48, pp. 2180–2184, Nov. 2000.

[35] O. P. Gandhi, G. Lazzi, and C. M. Furse, "Electromagnetic absorption in the human head and neck at 835 and 1900 MHz," *IEEE Trans. Microwave Theory Tech.*, vol. 44, pp. 1884–1887, Oct. 1996.

[36] G. Lazzi and O. P. Gandhi, "On modeling and personal dosimetry of cellular telephone helical antennas with the FDTD code," *IEEE Trans. Antennas Propagat.*, vol. 46, pp. 525–530, Apr. 1998.

[37] K. Miyamoto, J. Wang, and O. Fujiwara, "Relationship between temperature-rise in brain and localized SAR in anatomical head models of adult and children for portable telephone," in *Proc. IEICE General Conf.*, 2003, Paper B-4-3.

[38] W. A. Selle, *Body Temperature*. Springfield, IL: Charles C. Thomas, 1952.

Akimasa Hirata (S'99–A'00–M'01) was born in Okayama, Japan, on November 27, 1973. He received the B.E., M.E., and Ph.D. degrees in communication engineering from Osaka University, Suita, Osaka, Japan, in 1996, 1998, and 2000, respectively.

From 1999 to 2001, he was a Research Fellow of the Japan Society for the Promotion of Science (JSPS Research Fellow). From May to October 2000, he was also a Visiting Research Scientist with the University of Victoria, Victoria, BC, Canada. In 2001, he joined the Department of Communication Engineering, Osaka University, as a faculty member. His research interests are in electron beam devices for high-power millimeter or submillimeter generation, bioelectromagnetics, analysis of waveguides and filters, electromagnetic compatibility (EMC) in power engineering, and computational techniques in electromagnetics.

Dr. Hirata is a member of the Institute of Electrical, Information and Communication Engineers (IEICE), Japan. He was the recipient of the 1999 Institution of Electrical Engineers (IEE) Paper Presentation Award, the 2000 Research Encouragement Award presented at the Kansai Section Joint Convention of Institutes of Electrical Engineering, the 2001 URSI Commission B Young Scientist Award, the 2001 Ericsson Inc. Young Scientist Award, the 2001 IEEE Antennas and Propagation Society (IEEE AP-S) Tokyo Chapter Young Engineer Award, and the 2002 URSI GA Young Scientist Award.

Toshiyuki Shiozawa (S'64–M'69–SM'85–F'01) was born in Tokyo, Japan, on January 16, 1941. He received the B.E., M.E., and Ph.D. degrees in electrical communication engineering from Osaka University, Suita, Osaka, Japan, in 1964, 1966, and 1969, respectively.

In 1969, he joined the Department of Communication Engineering, Osaka University, where he is currently a Professor. He has been engaged in the research of relativistic EM theory for engineering-oriented applications and free-electron lasers in the millimeter- and submillimeter-wave regions. His current research interests include nonlinear electromagnetics and bioelectromagnetics. He coauthored *Topics in Advanced Electromagnetic Theory* (Tokyo, Japan: Corona, 1988) and *Electromagnetic Theory* (Tokyo, Japan: Corona, 1998). From 1995 to 1999, he served as an Associate Editor of the *IEICE Transactions on Electronics*.

Dr. Shiozawa is a member of the Institute of Electrical Engineers of Japan and the Institute of Electronics, Information and Communication Engineers (IEICE), Japan. He has served as a member of the Editorial Board of the IEEE TRANSACTIONS ON MICROWAVE THEORY AND TECHNIQUES. He was the chairman of the Technical Committee on Electromagnetic Theory in Institute of Electrical Engineers (IEE), Japan for the 1999–2002 period. In 2000, he organized the Japan–China Joint Meeting on Optical Fiber Science and Electromagnetic Theory (OFSET 2000).